

# Multi-Modal MPPI and Active Inference for Reactive Task and Motion Planning

Yuezhe Zhang, Corrado Pezzato, Elia Trevisan, Chadi Salmi, Carlos Hernández Corbato, Javier Alonso-Mora

**Abstract**—Task and Motion Planning (TAMP) has made strides in complex manipulation tasks, yet the execution robustness of the planned solutions remains overlooked. In this work, we propose a method for reactive TAMP to cope with runtime uncertainties and disturbances. We combine an Active Inference planner (AIP) for adaptive high-level action selection and a novel Multi-Modal Model Predictive Path Integral controller (M3P2I) for low-level control. This results in a scheme that simultaneously adapts both high-level actions and low-level motions. The AIP generates alternative symbolic plans, each linked to a cost function for M3P2I. The latter employs a physics simulator for diverse trajectory rollouts, deriving optimal control by weighing the different samples according to their cost. This idea enables blending different robot skills for fluid and reactive plan execution, accommodating plan adjustments at both the high and low levels to cope, for instance, with dynamic obstacles or disturbances that invalidate the current plan. We have tested our approach in simulations and real-world scenarios. Experiments’ videos are available at <https://sites.google.com/view/m3p2i-aip>.

## I. INTRODUCTION

Task and motion planning is a powerful class of methods for solving complex long-term manipulation problems where logic and geometric variables influence each other. TAMP [1] has been successfully applied to domains such as table rearrangement, stacking blocks, or solving the Hanoi tower. Despite impressive recent results [2], the environments in which TAMP is executed are usually not dynamic, and the plan is executed in open-loop [3]. Recent works [4]–[6] recognized the importance of robustifying the execution of TAMP plans to be able to carry them out in the real world reliably. However, they either rely only on the adaptation of the action sequence in a plan [6]–[9] or only on the motion planning problem in a dynamic environment given a fixed plan [4], [5]. This paper aims to achieve reactive execution by simultaneously adapting high-level actions and low-level motions.

A key challenge in reactive TAMP is handling geometric constraints that might not be known at planning time. For instance, moving a block to a desired location may necessitate pulling rather than pushing if the block is situated in a corner. Planning at the high level for these contingencies is hard especially when not assuming full knowledge of the scene at planning time. Another challenging scenario could be a

This research was supported by Ahold Delhaize. All content represents the opinion of the author(s), which is not necessarily shared or endorsed by their respective employers and/or sponsors.

The authors are with the Cognitive Robotics Department, TU Delft, 2628 CD Delft, The Netherlands [yuezhezhang\\_bit@163.com](mailto:yuezhezhang_bit@163.com), [{c.pezzato, e.trevisan, c.salmi, c.h.corbato, j.alonsomora}@tudelft.nl](mailto:{c.pezzato, e.trevisan, c.salmi, c.h.corbato, j.alonsomora}@tudelft.nl)

pick-and-place task with dynamic obstacles and human disturbances. Different grasping poses are necessary for diverse locations of the objects and obstacles. Thus, a TAMP algorithm should be able to adapt to these configurations on the fly.

We address these challenges by proposing a control scheme that jointly achieves reactive action selection and robust low-level motion planning during execution. We propose a high-level planner capable of providing alternative actions to achieve a goal. These actions are translated to different cost functions for our new Multi-Modal Model Predictive Path Integral controller for motion planning. This motion planner leverages a physics simulator to sample parallel motion plans that minimize the given costs and computes one coherent control input that effectively blends different strategies. To achieve this, we build upon two of our recent works: 1) an Active Inference planner (AIP) [7] for symbolic action selection, and 2) a Model Predictive Path Integral (MPPI) controller [10] for motion planning. We extend the previous AIP to plan possible alternative plans, and we propose a new Multi-Modal Model Predictive Path Integral controller (M3P2I) that can sample in parallel these alternatives and smoothly blend them.

## A. Related work

To robustly operate in dynamic environments, reactive motion planners are necessary. In [4], the authors provide a reactive MPC strategy to execute a TAMP plan as a given linear sequence of constraints. Instead of composing primitive skills, [4] derive the control law from a composition of constraints for MPC. The reactive nature of the approach allows coping with disturbances and dynamic collision avoidance during the execution of a TAMP plan. The work in [5] formulates a TAMP plan in object-centric Cartesian coordinates, showing how this allows coping with perturbations such as moving a target location. However, both [4], [5] do not consider adaptation at the symbolic action level if a perturbation invalidates the current plan.

Several papers focused on adapting and repairing high-level action sequences during execution. Authors in [11] propose representing robot task plans as robust logical-dynamical systems. The method can effectively adapt the logic plan to deal with external human disturbances. Similarly, [12] presented a method to coordinate control chains and achieve robust plan execution through plan switching and controller selection. A recent paper [13] proposes to use Monte Carlo Tree Search in combination with Isaac Gym to speed up task planning for multi-step object retrieval from clutter, where complex

physical interaction is required. This is a promising direction, but [13] only allows for high-level reasoning while executing pre-defined motions in an open loop. Works such as [6], [14] combined behavior trees and linear temporal logic to adapt the high-level plan to cope with cooperative or adversarial human operators, environment changes, or failures. In our previous work [7], Active Inference and behavior trees were combined to provide reactive action selection in long-term tasks in partially observable and dynamic environments. This method achieved hierarchical deliberation and continual online planning, making it particularly appealing for the problem of reactive TAMP at hand. In this paper, we extend [7] via bridging the gap to low-level reactive control by planning cost functions instead of symbolic actions.

At the lower level, Model Predictive Control (MPC) is a widely used approach [15]–[17]. However, most MPC methods rely on convexifying constraints and cost functions. Notably, manipulation tasks often involve discontinuous contacts that are hard to differentiate.

Sampling-based MPCs offer a promising alternative, such as MPPI [18], [19]. These algorithms can handle non-linearities, non-convexities, or discontinuities of the dynamics and costs. MPPI relies on sampling control input sequences and forward system dynamics simulation. The resulting trajectories are weighted according to their cost to approximate an optimal control input. In [20], the authors propose an ensemble MPPI to cope with model parameters uncertainty. Sampling-based MPCs are generally applied for single-skill execution, such as pushing or reaching a target point. As pointed out in the future work of [21], one could use a high-level agent to set the cost functions for the sampling-based MPC for long-horizon cognitive tasks. We follow this line of thought and propose a method to compose cost functions for long-horizon tasks reactively. Moreover, classical MPPI approaches can only keep track of one cost function at a time. This means the task planner should propose a single plan to solve the task. However, some tasks might present geometric ambiguities for which multiple plans could be effective, and selecting what strategy to pursue can only be determined by the motion planner based on the geometry of the problem.

## B. Contributions

The contribution is a reactive task and motion planning algorithm based on:

- A new Multi-Modal MPPI (M3P2I) capable of sampling in parallel plan alternatives to achieve a goal, evaluating them against different costs. This enables the smooth blending of alternative solutions into a coherent behavior instead of switching based on heuristics.
- An enhanced Active Inference planner capable of generating alternative cost functions for M3P2I.

## II. BACKGROUND

In this section, we present the background knowledge about the Active Inference planner and Model Predictive Path Integral Control to understand the contributions of this paper. We refer the interested reader to the original articles [7], [22], [23] for a more in-depth understanding of the single techniques.

### A. Active Inference Planner

The AIP is a high-level decision-making algorithm that relies on symbolic states, observations, and actions [7]. Each independent set of states in AIP is a factor, and the planner contains a total of  $n_f$  factors. For a generic factor  $f_j$  where  $j \in \mathcal{J} = \{1, \dots, n_f\}$ , it holds:

$$s^{(f_j)} = \left[ s^{(f_j,1)}, s^{(f_j,2)}, \dots, s^{(f_j,m^{(f_j)})} \right]^\top, \\ \mathcal{S} = \{s^{(f_j)} | j \in \mathcal{J}\} \quad (1)$$

where  $m^{(f_j)}$  is the number of mutually exclusive symbolic values a state factor can have, each entry of  $s^{(f_j)}$  is a real value between 0 and 1, and the sum of the entries is 1. This represents the current belief state.

The continuous state of the world  $x \in \mathcal{X}$  is discretized through a symbolic observer such that the AIP can use it. Discretized observations  $o$  are used to build a probabilistic belief about the symbolic current state. Assuming one set of observations per state factor with  $r^{(f_j)}$  possible values:

$$o^{(f_j)} = \left[ o^{(f_j,1)}, o^{(f_j,2)}, \dots, o^{(f_j,r^{(f_j)})} \right]^\top, \\ \mathcal{O} = \{o^{(f_j)} | j \in \mathcal{J}\} \quad (2)$$

The robot has a set of symbolic actions that can act then their corresponding state factor:

$$a_\tau \in \alpha^{(f_j)} = \{a^{(f_j,1)}, a^{(f_j,2)}, \dots, a^{(f_j,k^{(f_j)})}\}, \\ \mathcal{A} = \{\alpha^{(f_j)} | j \in \mathcal{J}\} \quad (3)$$

where  $k^{(f_j)}$  is the number of actions that can affect a specific state factor  $f_j$ . Each generic action  $a^{(f_j, \cdot)}$  has associated a symbolic name, *parameters*, *pre-* and *postconditions*:

$$\begin{array}{lll} \text{Action } a^{(f_j, \cdot)} & \text{Preconditions} & \text{Postconditions} \\ \text{action\_name (par)} & \text{prec}_{a^{(f_j, \cdot)}} & \text{post}_{a^{(f_j, \cdot)}} \end{array}$$

where  $\text{prec}_{a^{(f_j, \cdot)}}$  and  $\text{post}_{a^{(f_j, \cdot)}}$  are *first-order logic predicates* that can be evaluated at run-time. A logical predicate is a boolean-valued function  $\mathcal{B} : \mathcal{X} \rightarrow \{\text{true}, \text{false}\}$ . Finally, we define the logical state  $l^{(f_j)}$  as a one-hot encoding of  $s^{(f_j)}$ . The AIP computes the posterior distribution over  $p$  plans  $\pi$  through free-energy minimization [7]. The symbolic action to be executed by a robot in the next time step is the first action of the most likely plan, denoted with  $\pi_{\zeta,0}$ :

$$\zeta = \max(\underbrace{[\pi_1, \pi_2, \dots, \pi_p]}_{\pi^\top}), \quad a_{\tau=0} = \pi_{\zeta,0}. \quad (4)$$

### B. Model Predictive Path Integral Control

MPPI is a method for solving optimal stochastic problems in a sampling-based fashion [22], [23]. Let us consider the following discrete-time systems:

$$x_{t+1} = f(x_t, v_t), \quad v_t \sim \mathcal{N}(u_t, \Sigma), \quad (5)$$

where  $f$ , a nonlinear state-transition function, describes how the state  $x$  evolves over time  $t$  with a control input  $v_t$ .  $u_t$  and  $\Sigma$  are the commanded input and the variance, respectively.  $K$  noisy input sequences  $V_k$  are sampled and then applied

to the system to forward simulate  $K$  state trajectories  $Q_k$ ,  $k \in [0, K-1]$ , over a time horizon  $T$ . Given the state trajectories  $Q_k$  and a designed cost function  $C$  to be minimized, the total state-cost  $S_k$  of an input sequence  $V_k$  is computed by evaluating  $S_k = C(Q_k)$ . Finally, each rollout is weighted by the importance sampling weights  $w_k$ . These are computed through an inverse exponential of the cost  $S_k$  with tuning parameter  $\beta$  and normalized by  $\eta$ . For numerical stability, the minimum sampled cost  $\rho = \min_k S_k$  is subtracted, leading to:

$$w_k = \frac{1}{\eta} \exp\left(-\frac{1}{\beta}(S_k - \rho)\right), \quad \sum_{k=1}^K w_k = 1 \quad (6)$$

The parameter  $\beta$  is called *inverse temperature*. The importance sampling weights are finally used to approximate the optimal control input sequence  $U^*$ :

$$U^* = \sum_{k=1}^K w_k V_k \quad (7)$$

The first input  $u_0^*$  of the sequence  $U^*$  is applied to the system, and the process is repeated. At the next iteration,  $U^*$  is used as a warm-start, time-shifted backward of one timestep. Specifically, the second last input in the shifted sequence is also propagated to the last input. In this work, we build on top of our previous MPPI approach [10], where we employed IsaacGym as a dynamic model of the system to forward simulate trajectory rollouts.

### III. METHODOLOGY

The proposed method is depicted in Fig. 1. After a general overview, we discuss the three main parts of the scheme: *action planner*, *motion planner*, and *plan interface*.

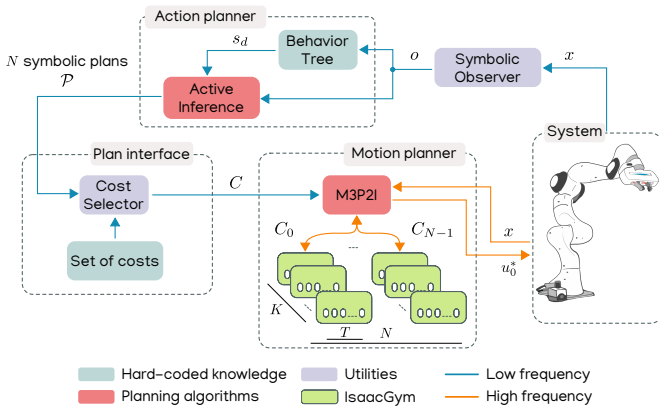


Fig. 1. Proposed scheme. Given symbolic observations  $o$  of the environment, the action planner computes  $N$  different plan alternatives linked to individual cost functions  $C_i$ . M3P2I samples control input sequences and uses an importance sampling scheme to approximate the optimal control  $u_0^*$ .

#### A. Overview

The proposed scheme works as follows. First, the *symbolic observers* translates continuous states  $x$  into discretized symbolic observations  $o$ . These are passed to a BT and Active Inference. The BT encodes the skeleton solution of a task in terms of desired states instead of actions as previous work [7]. The running node in a BT sets the current desired state  $s_d$  for

Active Inference. The latter computes  $N$  alternative symbolic plans based on the current symbolic state and the available symbolic actions. The symbolic actions are encoded as action templates with pre-post conditions that Active Inference uses to construct action sequences to achieve the desired state. After the plans are generated, the plan interface links the first action  $a_{0,i}$ ,  $i = 0 \dots N-1$  of each plan to a cost function  $C_i$ . The cost functions are sent to M3P2I, which samples  $N \cdot K$  different control input sequences. The input sequences are forward simulated using IsaacGym, which encodes the dynamics of the problem [10]. The resulting trajectories are evaluated against their respective costs. Finally, an importance sampling scheme calculates the approximate optimal control  $u_0^*$ . All processes are running continuously during execution at different frequencies. The action planner runs, for instance, at  $1Hz$  while the motion planner runs at  $25Hz$ . An overview can be found in Algorithm 1.

#### Algorithm 1 Overview of the method

```

1: while Task not completed do
2:    $o \leftarrow GetSymbolicObservation$ 
3:   /* Get current desired state from BT */
4:    $AIP.s_d \leftarrow BT$                                 ▷ from [7]
5:   /* Get current action plans from Active Inference */
6:    $\mathcal{P} \leftarrow AIP.parell\_act\_sel(o)$            ▷ Algorithm 2
7:   /* Translate action plan to cost function */
8:    $C \leftarrow Interface(\mathcal{P})$ 
9:   /* Compute motion commands */
10:   $M3P2I.command(C)$                                 ▷ Algorithm 4
11: end while

```

#### B. Action planner - Active Inference

The action planner we propose is a modified version of [7] to allow Active Inference to plan alternative action sequences to achieve a desired state. In contrast to our previous work [7] where only one action  $a_\tau$  for the next time step is computed, we modify the AIP to generate action alternatives. In particular, instead of stopping the search for a plan when a valid executable action  $a_\tau$  is found, we repeat the search while removing that same  $a_\tau$  from the available action set  $\mathcal{A}$ . This simple change is effective because we are looking for alternative actions to be applied at the next step, and the AIP builds plans backward from the desired state [7]. The pseudocode is reported in Algorithm 2. The algorithm will cease when no new actions are found, returning a list of possible plans  $\mathcal{P}$ . This planner is later integrated with the parallel motion planner M3P2I to evaluate different alternatives in real-time. This increases the robot's autonomy and performance, at the same time reducing the number of heuristics to be encoded in the action planner.

#### C. Motion planner - Multi-Modal MPPI (M3P2I)

We propose a Multi-Modal MPPI capable of sampling different plan alternatives from the AIP. Traditional MPPI approaches consider *one* cost function and *one* sampling distribution. In this work, we propose keeping track of  $N$  separate control input sequences corresponding to  $N$  different

**Algorithm 2** Generate alternative plans using Active Inference

---

```

1:  $a_\tau \leftarrow AIP.act\_sel(o)$                                  $\triangleright$  from [7]
2: Set  $\mathcal{P} \leftarrow \emptyset$ 
3: /* Look for alternatives */
4: while  $a_\tau \neq \text{none}$  do
5:    $\mathcal{P}.append(a_\tau)$ 
6:    $\mathcal{A} = \mathcal{A} \setminus \{a_\tau\}$ 
7:    $a_\tau \leftarrow AIP.act\_sel(o)$                                  $\triangleright$  from [7]
8: end while
9: Return  $\mathcal{P}$ 

```

---

plan alternatives/costs. This is advantageous because it offers a general approach to exploring different strategies in parallel. We perform  $N$  separate sets of importance weights, one for each alternative, and only ultimately, we combine the weighted control inputs in one coherent control. This allows the smooth blending of different strategies. Assume we consider  $N$  alternative plans, a total of  $N \cdot K$  samples. Assume the cost of plan  $i, i \in [0, N)$  to be formulated as:

$$S_i(V_k) = \sum_{t=0}^{T-1} \gamma^t C_i(x_{t,k}, v_{t,k}) \quad (8)$$

$\forall k \in \kappa(i)$  where  $\kappa(i)$  is the integer set of indexes ranging from  $i \cdot K$  to  $(i + 1) \cdot K - 1$ . State  $x_{t,k}$  and control input  $v_{t,k}$  are indexed based on the time  $t$  and trajectory  $k$ . The random control sequence  $V_k = [v_{0,k}, v_{1,k}, \dots, v_{T-1,k}]$  defines the control inputs for trajectory  $k$  over a time horizon  $T$ . The trajectory  $Q_i(V_k) = [x_{0,k}, x_{1,k}, \dots, x_{T-1,k}]$  is determined by the control sequence  $V_k$  and the initial state  $x_{0,k}$ .  $C_i$  is the cost function for plan  $i$ . Finally,  $\gamma \in [0, 1]$  is a discount factor that evaluates the importance of accumulated future costs. As in classical MPPI approaches, given the costs  $S_i(V_k)$ , we can compute the importance sampling weights associated with each alternative as:

$$\omega_i(V_k) = \frac{1}{\eta_i} \exp\left(-\frac{1}{\beta_i} (S_i(V_k) - \rho_i)\right), \forall k \in \kappa(i) \quad (9)$$

$$\eta_i = \sum_{k \in \kappa(i)} \exp\left(-\frac{1}{\beta_i} (S_i(V_k) - \rho_i)\right) \quad (10)$$

$$\rho_i = \min_{k \in \kappa(i)} S_i(V_k) \quad (11)$$

We use the insight in [10] to 1) sample Halton splines instead of Gaussian noise for smoother behavior, 2) automatically tune the inverse temperature  $\beta_i$  to maintain the normalization factor  $\eta_i$  within certain bounds. The latter is helpful since  $\eta_i$  indicates the number of samples to which significant weights are assigned. If  $\eta_i$  is close to the number of samples  $K$ , an unweighted average of sampled trajectories will be taken. If  $\eta_i$  is close to 1, then the best trajectory sample will be taken. We observed that setting  $\eta_i$  between 5% and 10% of  $K$  generates smooth trajectories. As opposed to [10], we update  $\eta$  *within a rollout* to stay within bounds instead of updating it once per iteration, see Algorithm 3. We use  $\mu_i$  to denote the action sequence of plan  $i$  over a time horizon

**Algorithm 3** Update inverse temperature  $\beta_i$ 


---

```

1: while  $\eta_i \notin [\eta_l, \eta_u]$  do
2:    $\rho_i \leftarrow \min_{k \in \kappa(i)} S_i(V_k);$                                  $\triangleright$  (11)
3:    $\eta_i \leftarrow \sum_{k \in \kappa(i)} \exp\left(-\frac{S_i(V_k) - \rho_i}{\beta_i}\right);$        $\triangleright$  (10)
4:   if  $\eta_i > \eta_u$  then                                 $\triangleright$  bigger than upper bound
5:      $\beta_i = 0.9 * \beta_i$ 
6:   else if  $\eta_i < \eta_l$  then       $\triangleright$  smaller than lower bound
7:      $\beta_i = 1.2 * \beta_i$ 
8:   end if
9: end while
10: Return  $\rho_i, \eta_i, \beta_i$ 

```

---

$\mu_i = [\mu_{i,0}, \mu_{i,1}, \dots, \mu_{i,T-1}]$ . Each sequence is weighted by the corresponding weights leading to:

$$\mu_i = \sum_{k \in \kappa(i)} \omega_i(V_k) V_k \quad (12)$$

At every iteration, we add to  $\mu_i$  the sampled noise from *Halton splines* [19]. Then, we forward simulate the state trajectories  $Q_i(V_k)$  using IsaacGym as in [10]. Finally, given the state trajectories corresponding to the plan alternatives, we need to compute the weights and mean for the overall control sequence. To do so, we concatenate the  $N$  state-costs  $S_i(V_k), i \in [0, N)$  and represent it as  $\tilde{S}(V)$ . Therefore, we calculate the weights for the whole control sequence as [19]:

$$\tilde{\omega}(V) = \frac{1}{\eta} \exp\left(-\frac{1}{\beta} (\tilde{S}(V) - \rho)\right) \quad (13)$$

Similarly,  $\eta, \rho$  are computed as in (10) and (11) but considering  $\tilde{S}(V)$  instead. The overall mean action over time horizon  $T$  is denoted as  $u = [u_0, u_1, \dots, u_{T-1}]$ . For each timestep  $t$ :

$$u_t = (1 - \alpha_u) u_{t-1} + \alpha_u \sum_{k=0}^{N \cdot K - 1} \tilde{\omega}_k(V) v_{t,k} \quad (14)$$

where  $\alpha_u$  is the step size that regularizes the current solution to be close to the previous  $u_{t-1}$ . The optimal control is set to  $u_0^* = u_0$ . Note that through (13), we can smoothly fuse different strategies to achieve a goal in a general way.

The pseudocode is summarized in Algorithm 4. After the initialization, we sample Halton splines and forward simulate the plan alternatives using IsaacGym to compute the costs (Lines 7-17). The costs are then used to update the weights for each plan and update their means (Lines 19-23). Finally, the mean of the overall action sequence is updated (Line 27), and the first action from the mean is executed.

*D. Plan interface*

The plan interface is a component that takes the possible alternative symbolic actions in  $\mathcal{P}$  and links them to their corresponding cost functions, forwarding the latter to M3P2I. For every symbolic action a robot can perform, we store a cost function in a database that we can query at runtime, bridging the output of the action planner to the motion planner.

**Algorithm 4** Multi-Modal Model Predictive Path Integral Control (M3P2I)

```

1: Parameters:  $N, K, T$ ;
2: Initialize:  $\mu_i = \mathbf{0}, u = \mathbf{0} \in \mathbb{R}^T \forall i \in [0, N]$ 
3: while task not completed do
4:    $x \leftarrow GetStateEstimate();$ 
5:    $InitIsaacGym(x)$ 
6:   /* Begin parallel sampling of alternatives */
7:   for  $i = 0$  to  $N - 1$  do
8:     for  $k \in \kappa(i)$  do
9:        $S_i(V_k) \leftarrow 0;$ 
10:      Sample noise  $\mathcal{E}_k \leftarrow SampleHaltonSplines();$ 
11:       $\mu_i \leftarrow BackShift(\mu_i);$ 
12:      for  $t = 0$  to  $T - 1$  do
13:         $Q_i(V_k) \leftarrow ComputeTrajIsaacGym(\mu_i + \mathcal{E}_k)$ 
14:         $S_i(V_k) \leftarrow UpdateCost(Q_i(V_k));$   $\triangleright (8)$ 
15:      end for
16:    end for
17:   end for
18:   /* Begin computing trajectory weights */
19:   for  $i = 0$  to  $N - 1$  do
20:      $\rho_i, \eta_i, \beta_i \leftarrow UpdateInvTemp(i);$   $\triangleright$  Algorithm 3
21:      $\omega_i(k) \leftarrow \frac{1}{\eta_i} \exp\left(-\frac{1}{\beta_i}(S_i(V_k) - \rho_i)\right), \forall k;$   $\triangleright (9)$ 
22:      $\mu_i = \sum_{k \in \kappa(i)} \omega_i(V_k) V_k$   $\triangleright (12)$ 
23:   end for
24:   /* Begin control update */
25:    $\tilde{\omega}(V) = \frac{1}{\eta} \exp\left(-\frac{1}{\beta}(\tilde{S}(V) - \rho)\right)$   $\triangleright (13)$ 
26:   for  $t = 0$  to  $T - 1$  do
27:      $u_t = (1 - \alpha_u)u_{t-1} + \alpha_u \sum_{j=0}^{N \cdot K - 1} \tilde{\omega}_k v_{t,k}$   $\triangleright (14)$ 
28:   end for
29:    $ExecuteCommand(u_0^* = u_0)$ 
30:    $u = BackShift(u)$ 
31: end while

```

#### IV. EXPERIMENTS

We evaluate the performance of our method in two different scenarios. The first is a *pull-push scenario* for non-prehensile manipulation of an object with an omnidirectional robot capable of both pulling and pushing. The second is the *object stacking scenario* with a 7-DOF manipulator with dynamic obstacles and external disturbances at runtime.

##### A. Push-pull scenario

This scenario is depicted in Fig. 2. One object has to be placed to a goal, situated in one of the corners of an arena. The object to be pushed can have different initial locations, for instance, in the middle of the arena or on one of the corners. There are also static and dynamic obstacles, and the robot can push or pull the object. We define the following action templates for the AIP and the cost functions for M3P2I.

1) *Action templates for AIP*: The AIP for this task requires one state  $s^{(goal)}$  and a relative symbolic observation  $o^{(goal)}$

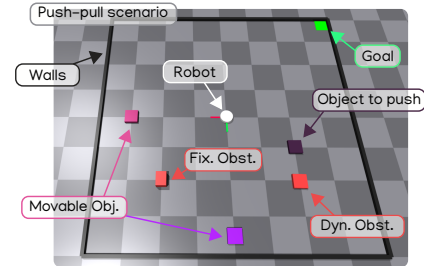


Fig. 2. Push-pull scenarios. The dark purple object has to be placed on the green area. The robot can pull or push the object while avoiding dynamic and fixed obstacles. The objects and goals can have different initial positions.

that indicates when an object is at the goal. This is defined as:

$$s^{(goal)} = \begin{bmatrix} \text{isAt(goal)} \\ \text{!isAt(goal)} \end{bmatrix}, o^{(goal)} = \begin{cases} 0, \|p_G - p_O\| \leq \delta \\ 1, \|p_G - p_O\| > \delta \end{cases} \quad (15)$$

where  $p_G, p_O$  represent the positions of the goal and the object in a 3D coordinate system.  $\delta$  is a constant threshold determined by the user. The mobile robot can either push, pull, or move. These skills are encoded in the action planner as follows:

Actions	Preconditions	Postconditions
push(obj, goal)	-	$l^{(goal)} = [1 \ 0]^\top$
pull(obj, goal)	-	$l^{(goal)} = [1 \ 0]^\top$

The post-condition of the action  $\text{push } (\text{obj}, \text{goal})$  is that the object is at the goal, similarly for the pull action. Note that we do not add complex heuristics to encode the geometric relations in the task planner to determine when to push or pull; instead, we will exploit parallel sampling in the motion planner later. The BT for this task sets  $s_d$  as a preference for  $l^{(goal)} = [1 \ 0]^\top$ . The BT would contain more desired states for pushing or pulling several blocks. Our approach can be extended to multiple objects in different locations, for instance, and accommodate more involved pre-post conditions and fallbacks since it has the same properties as in [7].

2) *Cost functions for MPPI*: We need to specify a cost for each symbolic action. The cost function for pushing object  $O$  to the goal  $G$  is defined as:

$$C_{\text{push}}(R, O, G) = C_{\text{dist}}(R, O) + C_{\text{dist}}(O, G) + C_{\text{ori}}(O, G) + C_{\text{align\_push}}(R, O, G) \quad (16)$$

where minimizing  $C_{\text{dist}}(O, G) = \omega_{\text{dist}} \cdot \|p_G - p_O\|$  makes the object  $O$  close to the goal  $G$ .  $C_{\text{ori}}(O, G) = \omega_{\text{ori}} \cdot \phi(\Sigma_O, \Sigma_G)$  defines the orientation cost between the object  $O$  and goal  $G$ . We define  $\phi$  for symmetric objects as:

$$\phi(\Sigma_u, \Sigma_v) = \min_{i,j \in \{1,2,3\}} (2 - \|\vec{u}_i \cdot \vec{v}_i\| - \|\vec{u}_2 \cdot \vec{v}_j\|) \quad (17)$$

where  $\Sigma_u = \{\vec{u}_1, \vec{u}_2, \vec{u}_3\}$ ,  $\Sigma_v = \{\vec{v}_1, \vec{v}_2, \vec{v}_3\}$  form the orthogonal bases of two coordinate systems. Minimizing this cost makes two axes in the coordinate systems of the object and goal coincide.

The align cost  $C_{align\_push}(R, O, G)$  is defined as:

$$C_{align\_push}(R, O, G) = \omega_{align\_push} \cdot h(\cos(\theta)), \quad (18)$$

$$\cos(\theta) = \frac{(p_R - p_O) \cdot (p_G - p_O)}{\|p_R - p_O\| \cdot \|p_G - p_O\|}, \quad (19)$$

$$h(\cos(\theta)) = \begin{cases} 0, & \cos(\theta) \leq 0 \\ \cos(\theta), & \cos(\theta) > 0 \end{cases} \quad (20)$$

This makes the object  $O$  lie at the center of robot  $R$  and goal  $G$  so that the robot can push it, as illustrated in Fig. 3.

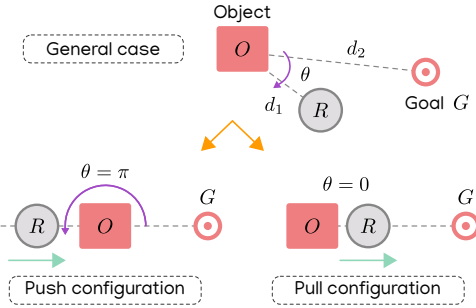


Fig. 3. Push and pull ideal configurations. The robot  $R$  has to push or pull the object  $O$  to the goal  $G$ .

Similarly, the cost function of making the robot  $R$  pull object  $O$  to the goal  $G$  can be formulated as:

$$C_{pull}(R, O, G) = C_{dist}(R, O) + C_{dist}(O, G) + C_{ori}(O, G) + C_{align\_pull}(R, O, G) + C_{act\_pull}(R, O, G) \quad (21)$$

where the align cost  $C_{align\_pull}(R, O, G)$  makes the robot  $R$  lie between the object  $O$  and goal  $G$ , see Fig. 3. While pulling, we simulate a suction force in IsaacGym, and we are only allowed to sample control inputs that move away from the object. We enforce this through  $C_{act\_pull}(R, O, G)$ . Mathematically:

$$C_{align\_pull}(R, O, G) = \omega_{align\_pull} \cdot h(-\cos(\theta)) \quad (22)$$

$$C_{act\_pull}(R, O, G) = \omega_{act\_pull} \cdot h\left(\frac{(p_O - p_R) \cdot \vec{u}}{\|p_O - p_R\| \cdot \|\vec{u}\|}\right) \quad (23)$$

An example execution of push and pull can be seen in Fig. 4. Finally, we consider an additional cost  $C_{dyn\_obs}(R, D)$  to avoid collisions with (dynamic) obstacles while operating. We use a constant velocity model to predict the position of the dynamic obstacle  $D$  in the coming horizon and try to maximize the distance between the latter and the robot:

$$C_{dyn\_obs}(R, D) = \omega_{dyn\_obs} \cdot e^{-\|p_R - p_{D_{pred}}\|} \quad (24)$$

where  $p_{D_{pred}}$  is the predicted position of dynamic obstacle.

3) *Results:* We test the performance of our multi-modal MPPI approach in two configurations of the arena: a) The object is in the middle of the arena, and the goal is to one corner, and b) both the object and the goals are in different corners. For each arena configuration, we test three cases: the robot can either only push, only pull, or combine the two through our M3P2I. At the beginning of the task,

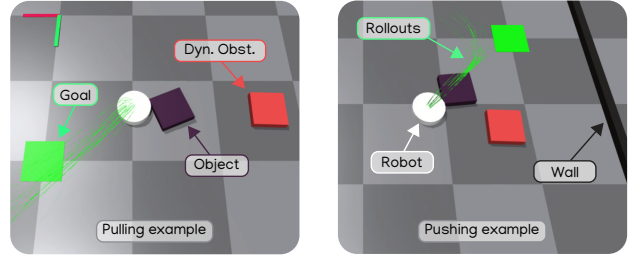


Fig. 4. Illustrative example of pulling and pushing a block to a goal. The strategy differs according to the object, goal location, and dynamic obstacle position. What action to perform is decided at runtime through multi-modal sampling.

the AIP plans for the two alternatives, pushing and pulling, and forwards the solution to the plan interface. Then, the M3P2I starts minimizing the costs until the AIP observes the completion of the task. We performed 20 trials per case, per arena configuration, for a total of 120 simulations. By only pulling an object, the robot cannot tightly place it on top of the goal in the corner; on the other hand, by only pushing, the robot cannot retrieve the object from the corner. By blending the push and pull actions, we can complete the task in every tested configuration. Table I shows that the multi-modal case outperforms push and pull in both arena configurations. It presents lower position and orientation errors and a shorter completion time. The behavior is best appreciated in the accompanying [video](#).

TABLE I  
SIMULATION RESULTS FOR PUSH AND PULL SCENARIO

Case	Skill	Mean(std) pos error	Mean(std) ori error	Mean(std) time
Middle-corner	Push	0.1061 (0.0212)	0.0198 (0.0217)	6.2058 (6.8084)
	Pull	0.1898 (0.0836)	0.0777 (0.1294)	25.1032 (13.7952)
	Multi-modal	<b>0.1052</b> (0.0310)	<b>0.0041</b> (0.0045)	<b>3.7768</b> (0.8239)
Corner-corner	Push	7.2679 (3.2987)	0.0311 (0.0929)	time-out
	Pull	0.3065 (0.1778)	0.1925 (0.2050)	32.8838 (7.9240)
	Multi-modal	<b>0.1375</b> (0.0091)	<b>0.0209</b> (0.0227)	<b>9.9473</b> (3.4591)

### B. Object stacking scenario

We now illustrate how we integrated the features of M3P2I with AIP's reactivity, enabling adjustments in both low-level motions and high-level actions. We address the challenge of stacking objects (Figure 5) with external task disruptions, necessitating adaptive actions like re-grasping with different pick configurations (e.g., top or side picking). We showcase the robot's ability to rectify plans by repeating actions or compensating for unplanned occurrences, such as unexpected obstacles obstructing the path. We benchmark our approach's performance against the cube-stacking task outlined in [24]. Our experiments employ a 7-DOF manipulator and include both simulation and real-world settings.

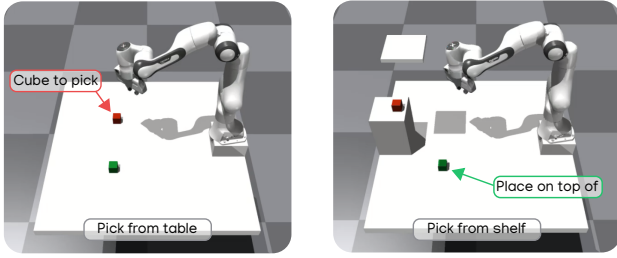


Fig. 5. Pick-place scenarios. The red cube has to be placed on top of the green cube. The red cube can be either on the table or a constrained shelf, requiring different pick strategies from the top or the side, respectively.

1) *Action templates for AIP*: For this task, we define the following states  $s^{(reach)}$ ,  $s^{(hold)}$ ,  $s^{(preplace)}$ ,  $s^{(placed)}$ , and their corresponding symbolic observations. The robot has four symbolic actions, summarized in Table II.

TABLE II  
ACTIONS WITH THEIR PRE AND POST CONDITIONS

Actions	Preconditions	Postconditions
reach(obj)	-	$l^{(reach)} = [1 \ 0]^\top$
pick(obj)	reachable(obj)	$l^{(hold)} = [1 \ 0]^\top$
prePlace(obj)	holding(obj)	$l^{(preplace)} = [1 \ 0]^\top$
place(obj)	atPreplace(obj)	$l^{(placed)} = [1 \ 0]^\top$

The symbolic observers to estimate the states are defined as follows. To estimate whether the gripper is close enough to the cube, we define the relative observation  $o^{(reach)}$ . We set  $o^{(reach)} = 0$  if  $\delta_r \leq 0.012$ , where  $\delta_r = ||p_{ee} - p_O||$  measures the distance between the end effector  $ee$  and the object  $O$ .  $o^{(reach)} = 1$  otherwise. To estimate whether the robot is holding the cube, we define:

$$o^{(hold)} = \begin{cases} 0, \delta_f < 0.065 \text{ and } \delta_f > 0.058 \\ 1, \delta_f \geq 0.065 \text{ or } \delta_f \leq 0.058 \end{cases} \quad (25)$$

where  $\delta_f = ||p_{ee\_l} - p_{ee\_r}||$  measures the distance between the two gripper's fingers. To estimate whether the cube reaches the pre-place location, we define:

$$o^{(preplace)} = \begin{cases} 0, C_{dist}(O, P) < 0.01 \text{ and } C_{ori}(O, P) < 0.01 \\ 1, C_{dist}(O, P) \geq 0.01 \text{ or } C_{ori}(O, P) \geq 0.01 \end{cases} \quad (26)$$

where  $C_{dist}(O, P)$  and  $C_{ori}(O, P)$  measure the distance and the orientation between the object  $O$  and the pre-place location  $P$  as in (16). The pre-place location is a few centimeters higher than the target cube location, directly on top of the green cube. We use the same logic as (26) for  $o^{(placed)}$  where the place location is directly on top of the cube location. The BT for this task sets the desired state to be  $s_d \rightarrow s^{(placed)} = [1 \ 0]^\top$ , meaning the cube is correctly placed on top of the other. Note that in more complex scenarios, such as rearranging many cubes, the BT can guide the AIP as demonstrated in [7].

2) *Cost functions for M3P2I*: At the motion planning level, the cost functions for the four actions are formulated as

follows:

$$C_{reach}(ee, O, \psi) = \omega_{reach} \cdot ||p_{ee} - p_O|| + \omega_{tilt} \cdot \left( \frac{||\vec{z}_{ee} \cdot \vec{z}_O||}{||\vec{z}_{ee}|| \cdot ||\vec{z}_O||} - \psi \right) \quad (27)$$

$$C_{pick}(ee) = \omega_{gripper} \cdot l_{gripper} \quad (28)$$

$$C_{preplace}(O, P) = C_{dist}(O, P) + C_{ori}(O, P) \quad (29)$$

$$C_{place}(O, P) = \omega_{gripper} \cdot (1 - l_{gripper}) \quad (30)$$

where  $C_{reach}(ee, O, \psi)$  makes the end effector get close to the object with a grasping tilt constraint  $\psi$ . When  $\psi$  is close to 1, the gripper will be perpendicular to the object; when  $\psi$  is close to 0, the gripper will be parallel to the plane that the object stands on.

3) *Results - reactive pick and place*: We first consider the pick-and-place under disturbances. We model disturbances by changing the position of the cubes at any time. We compare the performance of our method with the off-the-shelf RL method [24]. This is a readily available Actor-Critic RL example from IsaacGym, which considers the same tabletop configuration and robot arm. We compare the methods in a *vanilla* task without disturbances and a *reactive* task with disturbances. It should be noticed that the cube-stacking task in [24] only considers moving the cube on top of the other cube while neglecting the action of opening the gripper and releasing the cube. In contrast, our method exhibits fluent transitions between pick and place and shows robustness to interferences during the long-horizon task execution. The results can be found in Table III, where we performed 50 trials per case. Even though the RL agent presents a slightly lower position error in the *vanilla* case, our method outperforms it in the *reactive* task.

TABLE III  
SIMULATION RESULTS OF REACTIVE PICK AND PLACE

Task	Method	Training Epochs	Mean(std) pos error
Vanilla	Ours	0	0.0075 (0.0036)
	RL	1500	<b>0.0042</b> (0.0019)
Reactive	Ours	0	<b>0.0117</b> (0.0166)
	RL	1500	0.0246 (0.0960)

4) *Results: multi-modal grasping*: In this case, we consider grasping the object with different grasping poses by sampling two alternatives in parallel. That is, pick from the top or the side to cover the cases when the object is on the table or the constrained shelf with an obstacle above. To do so, we use the proposed M3P2I and incorporate the cost functions of  $C_{reach}(ee, O, \psi = 0)$  and  $C_{reach}(ee, O, \psi = 1)$  as shown in (27). This allows for a smooth transition between op and side grasp according to the geometry of the problem, see Fig. 6.

5) *Results - real-world experiments*: We validate our method in the real world for reactive pick-and-place as shown in Fig. 7. We consider dynamic obstacles with a stick to be avoided and other human disturbances such as moving, rotating, and stealing the cube from the gripper. M3P2I enables smooth execution and recovery while being able to grasp the cube in different configurations.

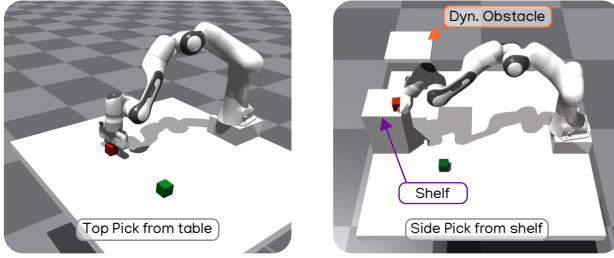


Fig. 6. Example of different picking strategies computed by our multi-modal MPPI. The obstacle on top of the shelf can be moved, simulating a dynamic obstacle. See the accompanying [video](#) for the actual execution.

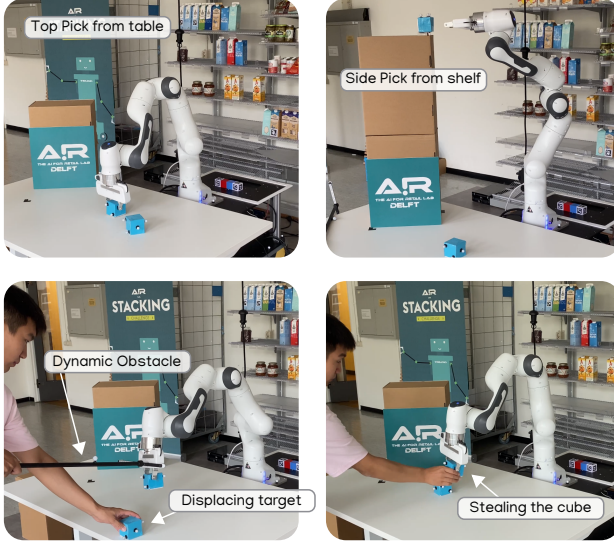


Fig. 7. Real-world experiments of picking a cube from the table or the shelf while avoiding dynamic obstacles and recovering from task disturbances. See the accompanying [video](#) for the actual execution.

## V. CONCLUSIONS

In this paper, to address the runtime geometric uncertainties and disturbances, we proposed a method to combine the adaptability of an Active Inference planner for high-level action selection with a novel Multi-Modal Model Predictive Path Integral Controller (M3P2I) for low-level control. We modified Active Inference to generate plan alternatives that are linked to costs for M3P2I. The motion planner can sample the plan alternatives in parallel, and it computes the control input for the robot by smoothly blending different strategies. In a push-pull task, we demonstrated how our proposed framework can blend both push and pull actions, allowing it to deal with corner cases where approaches only using a single plan fail. With a simulated manipulator, we showed our method outperforming a reinforcement learning baseline when the environment is disturbed while requiring no training. Simulated and real-world experiments demonstrated how our approach solves reactive object stacking tasks with a manipulator subject to severe disturbances and various scene configurations that require different grasp strategies.

## REFERENCES

- [1] C. R. Garrett, R. Chitnis, R. Holladay, B. Kim, T. Silver, L. P. Kaelbling, and T. Lozano-Pérez, “Integrated task and motion planning,” *Annual review of control, robotics, and autonomous systems*, vol. 4, 2021.
- [2] J. Ortiz-Haro, E. Karpas, M. Katz, and M. Toussaint, “A conflict-driven interface between symbolic planning and nonlinear constraint solving,” *IEEE RA-L*, vol. 7, no. 4, 2022.
- [3] C. R. Garrett, T. Lozano-Pérez, and L. P. Kaelbling, “Pddlstream: Integrating symbolic planners and blackbox samplers via optimistic adaptive planning,” in *Proceedings of the International Conference on Automated Planning and Scheduling*, vol. 30, 2020.
- [4] M. Toussaint, J. Harris, J.-S. Ha, D. Driess, and W. Höning, “Sequence-of-constraints mpc: Reactive timing-optimal control of sequential manipulation,” *IEEE IROS*, 2022.
- [5] T. Migmatsu and J. Bohg, “Object-centric task and motion planning in dynamic environments,” *IEEE RA-L*, vol. 5, no. 2, 2020.
- [6] S. Li, D. Park, Y. Sung, J. A. Shah, and N. Roy, “Reactive task and motion planning under temporal logic specifications,” in *2021 IEEE ICRA*. IEEE, 2021.
- [7] C. Pezzato, C. Hernandez, S. Bonhof, and M. Wisse, “Active inference and behavior trees for reactive action planning and execution in robotics,” *IEEE T-RO*, 2023.
- [8] N. Castaman, E. Pagello, E. Menegatti, and A. Pretto, “Receding horizon task and motion planning in changing environments,” *Robotics and Autonomous Systems*, vol. 145, 2021.
- [9] M. Colledanchise, D. Almeida, M., and P. Ögren, “Towards blended reactive planning and acting using behavior tree,” in *IEEE International Conference on Robotics and Automation (ICRA)*, 2019.
- [10] C. Pezzato, C. Salmi, M. Spahn, E. Trevisan, J. Alonso-Mora, and C. Hernández, “Sampling-based model predictive control leveraging parallelizable physics simulations,” *arXiv arXiv:2307.09105*, 2023.
- [11] C. Paxton, N. Ratliff, C. Eppner, and D. Fox, “Representing robot task plans as robust logical-dynamical systems,” in *2019 IEEE/RSJ IROS*, 2019.
- [12] J. Harris, D. Driess, and M. Toussaint, “FC<sup>3</sup>: Feasibility-based control chain coordination,” in *International Conference on Intelligent Robots and Systems (IROS)*, 2022.
- [13] B. Huang, A. Boulias, and J. Yu, “Parallel monte carlo tree search with batched rigid-body simulations for speeding up long-horizon episodic robot planning,” in *The IEEE/RSJ International Conference on Intelligent Robots and Systems (IROS)*. IEEE, 2022.
- [14] Z. Zhou, D. J. Lee, Y. Yoshinaga, S. Balakirsky, D. Guo, and Y. Zhao, “Reactive task allocation and planning for quadrupedal and wheeled robot teaming,” in *2022 IEEE 18th International Conference on Automation Science and Engineering (CASE)*, 2022.
- [15] M. Bangura and R. Mahony, “Real-time model predictive control for quadrotors,” *IFAC Proceedings Volumes*, vol. 47, no. 3, 2014.
- [16] N. Scianca, D. De Simone, L. Lanari, and G. Oriolo, “Mpc for humanoid gait generation: Stability and feasibility,” *IEEE T-RO*, 2020.
- [17] M. Spahn, B. Brito, and J. Alonso-Mora, “Coupled mobile manipulation via trajectory optimization with free space decomposition,” in *2021 IEEE ICRA*. IEEE, 2021.
- [18] G. Williams, N. Wagener, B. Goldfain, P. Drews, J. M. Rehg, B. Boots, and E. A. Theodorou, “Information theoretic mpc for model-based reinforcement learning,” in *2017 IEEE ICRA*. IEEE, 2017.
- [19] M. Bhardwaj, B. Sundaralingam, A. Mousavian, N. D. Ratliff, D. Fox, F. Ramos, and B. Boots, “Storm: An integrated framework for fast joint-space model-predictive control for reactive manipulation,” in *Conference on Robot Learning*. PMLR, 2022.
- [20] I. Abraham, A. Handa, N. Ratliff, K. Lowrey, T. D. Murphey, and D. Fox, “Model-based generalization under parameter uncertainty using path integral control,” *IEEE RA-L*, vol. 5, no. 2, 2020.
- [21] T. Howell, N. Gileadi, S. Tunyasuvunakool, K. Zazka, T. Erez, and Y. Tassa, “Predictive sampling: Real-time behaviour synthesis with mujoco,” *arXiv arXiv:2212.00541*, 2022.
- [22] G. Williams, A. Aldrich, and E. A. Theodorou, “Model Predictive Path Integral Control: From Theory to Parallel Computation,” *Journal of Guidance, Control, and Dynamics*, vol. 40, no. 2, Feb. 2017.
- [23] G. Williams, P. Drews, B. Goldfain, J. M. Rehg, and E. A. Theodorou, “Information-Theoretic Model Predictive Control: Theory and Applications to Autonomous Driving,” *IEEE T-RO*, 2018.
- [24] V. Makoviychuk, L. Wawrzyniak, Y. Guo, M. Lu, K. Storey, M. Macklin, D. Hoeller, N. Rudin, A. Allshire, A. Handa *et al.*, “Isaac gym: High performance gpu-based physics simulation for robot learning,” *arXiv arXiv:2108.10470*, 2021.